Original Article on Translational Imaging in Cancer Patient Care

Diffusion kurtosis imaging in assessment of gastric cancer aggressiveness

Changfeng Ji[1*], Yujuan Zhang[1*], Huanghuang Zheng[1], Ling Chen[2], Wenxian Guan[3], Tingting Guo[4], Qinglei Zhang[1], Song Liu[1], Jian He[1], Zhengyang Zhou[1]

[1]Department of Radiology, [2]Department of Pathology, [3]Department of Gastrointestinal Surgery, Nanjing Drum Tower Hospital, The Affiliated Hospital of Nanjing University Medical School, Nanjing 210008, China; [4]Department of Radiology, Nanjing Drum Tower Hospital, Clinical College of Traditional Chinese and Western Medicine, Nanjing University of Chinese Medicine, Nanjing 210008, China

Contributions: (I) Conception and design: S Liu, J He, Z Zhou; (II) Administrative support: Z Zhou; (III) Provision of study materials or patients: L Chen, W Guan; (IV) Collection and assembly of data: C Ji, Y Zhang, H Zheng, T Guo; (V) Data analysis and interpretation: C Ji, Y Zhang, S Liu; (VI) Manuscript writing: All authors; (VII) Final approval of manuscript: All authors.

*These authors contributed equally to this work.

Correspondence to: Song Liu, MD. No. 321 Zhongshan Road, Nanjing 210008, China. Email: liusongnj@126.com; Jian He, MD, PhD. No. 321 Zhongshan Road, Nanjing 210008, China. Email: hjxueren@126.com; Zhengyang Zhou, MD, PhD. No. 321 Zhongshan Road, Nanjing 210008, China. Email: zyzhou@nju.edu.cn.

Background: Diffusion kurtosis imaging (DKI) has been utilized in various tumors. The potential associations between parameters derived from DKI and the aggressiveness of gastric cancers are still unclear.

Methods: Forty-nine patients with gastric cancers were enrolled in this prospective study. All patients underwent magnetic resonance (MR) examination before surgery. All MR images were reviewed by two radiologists using software IDL 6.3 and an oval region of interest (ROI) was manually drawn on the specific slice showing the largest area of tumor. Three parameters were calculated automatically: apparent diffusion coefficient (ADC), corrected diffusion coefficient (diffusivity) and excess diffusion kurtosis coefficient (kurtosis).

Results: Poorly/moderate-poorly differentiated gastric cancers showed significantly lower ADC and higher kurtosis compared with moderately/well differentiated tumors (P=0.039, 0.002, respectively). Kurtosis was also significantly different in different Lauren classifications (P=0.010). ADC and diffusivity were significantly lower while kurtosis was significantly higher in gastric cancers with T3–T4 stages than in those with T1–T2 stages (P=0.004, 0.021, 0.009, respectively). Lower ADC and diffusivity were also observed in gastric cancers with N1–N3 stages (P=0.010, 0.023, respectively). No significant differences were found for ADC, diffusivity and kurtosis among different status of vascular invasion and perineural invasion.

Conclusions: DKI derived parameters might be helpful in preoperative assessment of gastric cancer's aggressiveness, especially in identifying poorly/moderate-poorly differentiated or diffuse type gastric cancers, and in predicting the status of lymph nodes metastasis.

Keywords: Aggressiveness; diffusion kurtosis imaging (DKI); magnetic resonance imaging (MRI); stomach neoplasm

Submitted Feb 06, 2017. Accepted for publication Jun 29, 2017.
doi: 10.21037/tcr.2017.07.02
View this article at: http://dx.doi.org/10.21037/tcr.2017.07.02

Introduction

Gastric cancer is one of the most common malignancies in the gastrointestinal tract, with high morbidity and mortality worldwide (1,2). Histopathological features of gastric cancers, including TNM stage, histological differentiation, Lauren classification, the status of vascular and perineural invasion, etc., are important prognostic factors and influence clinical treatment strategies vitally for gastric cancers (2-6). Therefore, the preoperative evaluation of those features is regard as essential and considerable. Currently, preoperative evaluation of gastric cancers mainly depends on endoscopic biopsy, while endoscopy is considered invasive accompanied by sampling error (7,8). Computed tomography (CT) has become routine preoperative imaging examination for patients with gastric cancers, but CT has ionizing radiation, relatively lower soft tissue resolution and offering less functional information.

Magnetic resonance imaging (MRI), a non-invasive examination without ionizing-radiation providing both morphological and functional information, has been increasingly utilized in preoperative assessment of gastric cancers, especially diffusion weighted imaging (DWI) (9-11). Apparent diffusion coefficient (ADC) is an important parameter of DWI, reflecting the diffusion of water molecules in tissues. Several studies have reported that ADC may be useful in assessing the aggressiveness of gastric cancers, such as TNM stage, histological differentiation, Lauren classification, etc. (12-15). However, traditional DWI is based on free diffusion of water molecules, while the microenvironments of tumors are complex, resulting in non-free diffusion of water molecules, namely non-Gaussian diffusion. Besides, traditional ADC value is usually calculated using a mono-exponential model, which might be influenced by the microvascular circulation in tissues (16,17). Expanded DWI with multiple b values, including diffusion kurtosis imaging (DKI) and intravoxel incoherent motion imaging has showed great potential in tumor evaluation and hepatic fibrosis (16-20). DKI is a new functional imaging technique proposed by Jensen *et al.* in 2005, which could describe non-Gaussian distribution of water molecules in tissues (21). DKI mainly includes two parameters, kurtosis and diffusivity. Kurtosis reflects the deviation of water diffusion from the Gaussian distribution, while diffusivity is the diffusion coefficient with the correction of non-Gaussian distribution bias. In recent years, DKI has been initially used in a variety of tumors, such as glioma, rectal cancer, prostate cancer, etc. (20,22-25). Yu *et al.* served DKI as a valuable tool in assessing treatment response of neoadjuvant chemoradiotherapy in locally advanced rectal cancer (26). Jiang *et al.* demonstrated that DKI may be a noninvasive method for the differentiation between benign and malignant sinonasal lesions (27). In addition, several studies have also demonstrated that DKI is superior to traditional DWI in assessing tumor aggressiveness (20,22,23). For example, Zhu *et al.* reported in their study that kurtosis derived from DKI demonstrated significant correlation with histologic grades of rectal cancers on the basis of poorly differentiated clusters, and performed better than ADC from DWI in differentiating between high- and low-grade rectal carcinomas (20). Authors of a recent study about breast cancer also demonstrated that kurtosis and diffusivity from DKI showed significantly higher specificity for differentiation of malignant from benign breast lesions than ADC from DWI; moreover, kurtosis and diffusivity were significantly correlated with histological grade and expression of the Ki-67 protein in breast cancers, while ADC from DWI showed no significant correlations (23).

However, to our limited knowledge, no studies reported the utility of DKI-derived parameters in assessment of gastric cancers. Thus, the purpose of this study was to evaluate the potential associations between parameters derived from DKI and the aggressiveness of gastric cancers.

Methods

Patients

This prospective study received the approval of local ethics committee. Written informed consent was obtained from each patient. Patients who satisfied the following criteria were potentially included in our study: (I) with a diagnosis of gastric cancer confirmed by endoscopic biopsy; (II) willing to undergo MR examination for preoperative assessment; (III) without absolute contraindications to MR examination and gadolinium contrast agents, such as cardiac pacemaker or defibrillator, aneurysm clip, nerve stimulator, insulin pump, cochlear implant. The exclusion criteria were as follows: (I) receiving local or systematic treatment before MR examination or surgery; (II) without accurate postoperative histopathological information (including histological differentiation, Lauren classification, vascular invasion, perineural invasion and TNM stage, etc.); (III) with a minimum diameter of tumor less than 5 mm

insufficient to contain a region of interest (ROI) for image analyses; (IV) poor MR image quality for further analysis due to motion or magnetic susceptibility artifacts. A detailed inclusion and exclusion flowchart is shown in *Figure 1*.

From Dec. 2015 to Nov. 2016, a total of 49 patients with gastric cancers were finally enrolled in this study. The study cohort was comprised of 31 men and 18 women (age range, 28–84 years; mean age ± standard deviation, 62±12 years).

MR examination

All patients underwent MR examination after fasting over 8 h. After confirming that no contraindications (such as glaucoma, prostate hypertrophy or severe heart disease) were presented, 20 mg of scopolamine butylbromide (1 mL: 20 mg; Chengdu NO.1 Drug Research Institute Company Limited, Chengdu, China) was injected intramuscularly to prevent gastrointestinal motility 10 minutes before MR examination. Forty-one (83.7%) of 49 patients received scopolamine butylbromide (no adverse effects occurred during or after MR examination), whereas the remaining 8 patients (16.3%) had a contradiction to the drug regimen (6 patients) or rejected the drug (2 patients). Then all patients were asked to drink 800–1000 mL water 10 minutes before MR examination to fill the gastric cavity. Before MR scanning, the patients were trained to breathe smoothly.

All MR images were collected by using a clinical whole body 3.0 T scanner (Ingenia 3.0 T; Philips Medical Systems, Best, the Netherlands) with a 32 channels dStream Torso coil. Patients were placed in a supine position with head first. The respiratory sensor was carefully placed between the patient and coil. Scan duration per respiration and respiratory trigger delay were fit into the expiration phase of each patient's respiratory cycle. The maximum gradient strength and slew rate of the MR scanner system were 45 mT/s and 200 mT/m/s, respectively. MR sequences included axial T2 weighted (T2W) images, T1 high resolution isotropic volume excitation (THRIVE) and axial respiratory-triggered single-shot echo-planar DKI: Axial T2W images were obtained with respiratory-triggered turbo spin-echo sequence without fat-saturation (repetition time =1,000 ms, echo time =80 ms, field of view =380 mm × 380 mm, matrix =308×252, section thickness =5 mm, intersection gap =0.5 mm, number of signal averages =2, and bandwidth =534.0 Hz/pixel).

THRIVE with breath-holding and spectral attenuated inversion recovery techniques (repetition time =3.00 ms, echo time =1.42 ms, field of view =380 mm × 380 mm, matrix =224×194, section thickness =5 mm, intersection gap =0.5 mm; number of signal averaged =1, and bandwidth =715.4 Hz/pixel) were utilized before and 30, 60, 90, and 180 seconds after administration of 0.2 mL per kilogram of body weight gadodiamide (Omniscan 0.5 mmol/mL; GE Healthcare, Ireland) using an automatic power injector (Medrad Spectris Solaris EP MR Injector System; One Medrad Drive Indianola, PA, US).

Axial respiratory-triggered single-shot echo-planar DKI sequence used five b values of 0, 500, 1,000, 1,500 and 2,000 s/mm^2 and the numbers of signal averages were one average (b value of 0–499 s/mm^2), two averages (b value of 500–1,499 s/mm^2) and three averages (b value of 1,500–2,000 s/mm^2). Other parameters were as follows: repetition time =8,000 ms, echo time =65 ms, field of view =360 mm × 300 mm, matrix =116×100, section thickness =5 mm, intersection gap =0.5 mm, parallel imaging factor =4 and bandwidth =2,665.9 Hz/pixel. The spectral presaturation with inversion recovery fat suppression technique was used for DKI sequence. There were three motion probe gradient directions, which were frequency encoding, phase encoding and slice choosing directions, respectively.

Image analyses

All MR images were reviewed by two radiologists (Jian He, Zhengyang Zhou) with 8 and 10 years' experience in abdominal radiology, who were blinded to the endoscopic biopsy and postoperative pathologic findings. The DKI sequence was loaded into software IDL 6.3 (ITT Visual Information Solutions, Boulder, CO). The parameters diffusivity and kurtosis were calculated using a kurtosis-imaging model (21): $S_i = S_0 \times \exp(-b_i \times D + 1/6 \times b_i^2 \times D^2 \times K)$, where S_i is the signal intensity at b value = b_i, S_0 is the signal intensity at b =0, D (diffusivity) is corrected diffusion coefficient and K (kurtosis) is diffusion kurtosis coefficient. The ADC value was calculated with a mono-exponential decay model: $S_i = S_0 \times \exp(-b_i \times ADC)$, where S_i is the signal intensity at b value = b_i, S_0 is the signal intensity at b =0 and ADC is the ADC. Additionally, the tumor volume of each patient was also measured and recorded.

Gastric cancer lesions showed thickened wall on T2W images and hyperintense on DKI (b =1,000 s/mm²) with remarkable contrast enhancement. For each patient, the specific slice of axial DKI (b =1,000 s/mm²) showing the

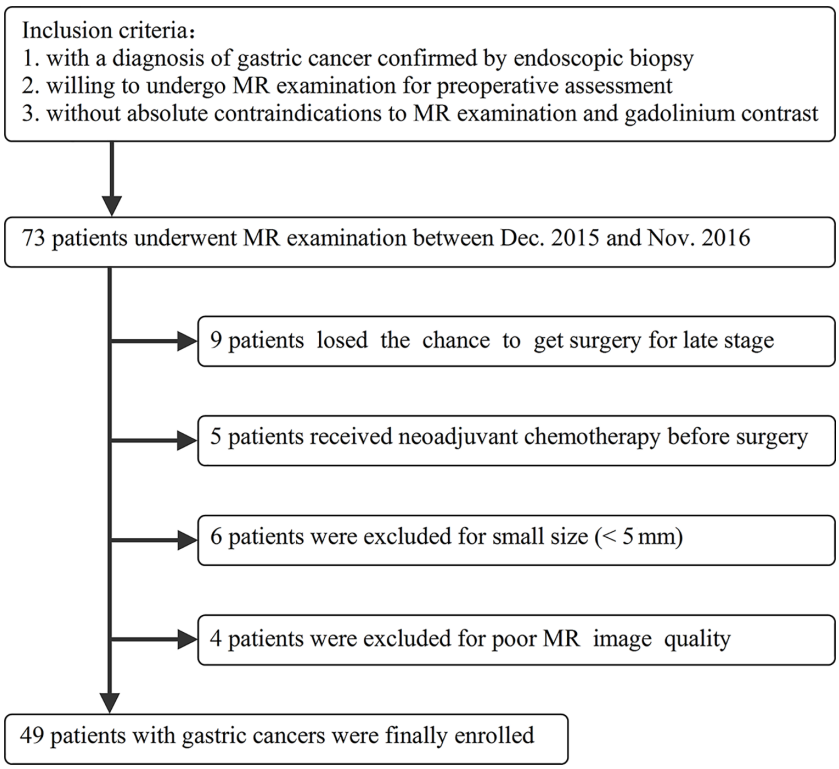

Figure 1 Inclusion and exclusion flowchart of this study.

largest area of tumor was selected. Based on the consensus of two radiologists, an oval ROI was manually drawn as large as possible within the solid part of the lesion by referring to the corresponding images of other MR sequences. If the lesion showed a sandwich sign (28), the ROI was set to avoid the internal muscular layer. The ROI was automatically transferred into the parameter maps and the mean value from each ROI was obtained.

Postoperative histopathological analyses

Forty-two patients underwent curative gastrectomy (including 16 total and 26 partial gastrectomies) and 7 patients underwent palliative resection by the surgeons (Meng Wang, Hao Wang) with 6- and 9-year experience in gastrointestinal surgery. The pathological analyses were performed by a pathologist (Ling Chen) with 6-year experience in digestive malignancy, who was blinded to MR findings and DKI measurements. The histological differentiation, Lauren classification, vascular invasion, perineural invasion and TNM stage of the gastric cancers were analyzed and recorded according to the World Health Organization (WHO) classification [2010] and the TNM classification of the American Joint Committee on Cancer (AJCC, 7th edition) (29,30).

Statistical analyses

Shapiro-Wilk tests were used to check normality assumption for all parameters in all groups ($P<0.05$ indicated non-normal distribution). Quantitative values in normal distribution were presented as mean ± standard deviation, while those in non-normal distribution were presented as median (interquartile range).

One-way analysis of variance (normality) or Kruskal-Wallis test (non-normality) was used to detect the differences of ADC, diffusivity and kurtosis among gastric cancers with different Lauren classifications and N stages.

Independent samples *t*-test (normality) or Mann-Whitney U test (non-normality) was used to compare ADC, diffusivity and kurtosis between different differentiation degrees (poorly/moderate-poorly *vs.* moderately/well),

T stages (T1–T2 *vs.* T3–T4), N stages (N0 *vs.* N1–N3), vascular invasion (present *vs.* absent) and perineural invasion (present *vs.* absent).

Correlations between tumor volume and differentiation degree (poor, moderate-poor, moderate and well), Lauren classification, T stage (T1–T4), N stage (N0–N3) and overall stage of gastric cancers were evaluated by using Spearman correlation test while correlations between tumor volume and DKI parameters were analyzed by Pearson correlation test. Correlations between DKI parameters (ADC, diffusivity and kurtosis) with differentiation degree (poor, moderate-poor, moderate and well), Lauren classification, T stage (T1–T4), N stage (N0–N3) and overall stage of gastric cancers were evaluated with partial correlation test to remove the impact due to tumor size (correlation coefficient r, 0.000–0.300, weak; 0.301–0.500, moderate; 0.501–0.800, strong; 0.801–1.000, very strong).

Diagnostic performance of the ADC, diffusivity and kurtosis in differentiating gastric cancers with poor differentiation degree, at N1–N3 stages or of diffuse type was tested with receiver operating characteristic (ROC) curve analysis. The cutoff values with the largest Youden index (sensitivity + specificity −1) were calculated from the ROC curves.

All statistical analyses were performed with SPSS (version 22.0 for Microsoft Windows ×64, SPSS, US). A two-tailed P value less than 0.05 was considered statistically significant.

Results

The clinicopathological characteristics of all the 49 patients with gastric cancers are shown in *Table S1*, and one lesion was identified in each patient. The tumor volume of these patients ranged from 812.50 to 142,635.00 mm^3, with the average volume of 35,115.88±34,157.40 mm^3. A representative case of gastric cancer is shown in *Figure 2*.

One-way analysis of variance and independent samples t test

The values of ADC, diffusivity and kurtosis followed normal distribution in all groups with Shapiro-Wilk tests (*Table S1*). Poorly/moderate-poorly differentiated gastric cancers showed significantly lower ADC and higher kurtosis compared with moderately/well differentiated tumors. Kurtosis was also significantly different in different Lauren classifications. ADC and diffusivity were significantly lower while kurtosis was significantly higher in gastric cancers with T3–T4 stages than in those with T1–T2 stages. Lower ADC and diffusivity were also observed in gastric cancers with N1–N3 stages. No significant differences were found for ADC, diffusivity and kurtosis among different status of vascular invasion and perineural invasion (*Table 1*).

ROC curve analysis

ADC and kurtosis could differentiate poorly/moderate-poorly differentiated gastric cancers from moderately/well differentiated ones with an AUC value of 0.732 and 0.794, respectively. Kurtosis could also differentiate diffuse type gastric cancers from mixed/intestinal types with an AUC of 0.737. ADC and diffusivity performed well in differentiating gastric cancers with and without lymph node metastasis with an AUC of 0.741 and 0.729, respectively (*Figure 3*, *Table 2*).

Correlation analysis

There were significant correlations between tumor volume and differentiation degree, Lauren classification, T stage, N stage and overall stage of gastric cancers (r= −0.347, −0.330, 0.564, 0.333 and 0.474, respectively, all P values <0.05) while no significant correlations were found between tumor volume and DKI parameters (r= −0.209, −0.208 and 0.196 for ADC, diffusivity and kurtosis, respectively, all P values >0.05). ADC correlated positively while kurtosis correlated negatively with differentiation degree (r=0.372 and −0.481, respectively) and Lauren classification of gastric cancers (r=0.287 and −0.388, respectively). Diffusivity and ADC correlated negatively while kurtosis correlated positively with T stages of gastric cancers (r= −0.322, −0.394 and 0.330, respectively). ADC correlated negatively while kurtosis correlated positively with overall stages of gastric cancers (r= −0.341 and 0.306, respectively) (*Table 3*).

Discussion

Our study initially confirmed the feasibility of DKI in the evaluation of gastric cancerous aggressiveness. We found that DKI parameters could help to assess the differentiation degree, Lauren classification, T stage and the status of lymph nodes metastasis of gastric cancers, which has never been reported previously.

Poor differentiation degree is a predictor of poor

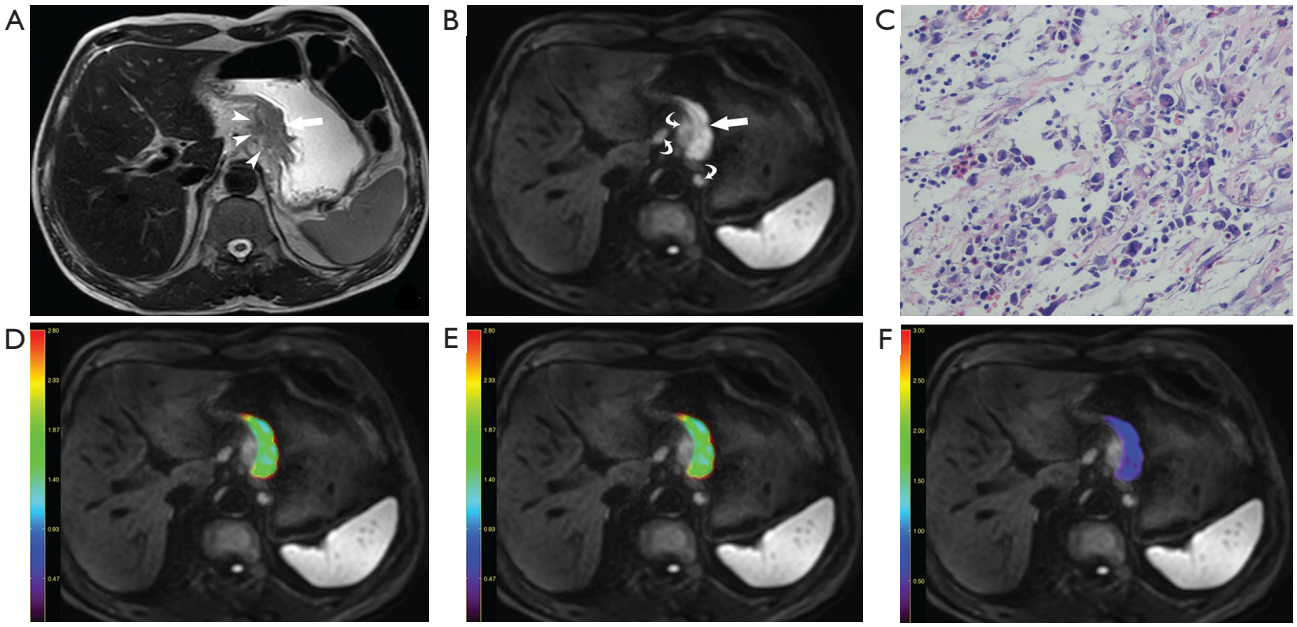

Figure 2 A 65-year-old man with gastric cancer pathologically diagnosed at stage T4N3. (A) Axial T2 weighted image shows a thickened wall in stomach cardia (arrow) extending into surrounding fat spaces (arrow heads); (B) axial diffusion kurtosis image (b =1,000 s/mm^2) shows the lesion with remarkably high signal intensity and multiple enlarged metastatic lymph nodes around (curved arrows); (C) the photomicrograph (Hematoxylin & Eosin staining, 200×) shows a poorly cohesive carcinoma (mixed with approximately 20% mucinous adenocarcinoma) with a Lauren classification of diffuse type; (D) ADC; (E) corrected diffusion coefficient (D) and (F) diffusion kurtosis coefficient (K) color maps fused with (B) show that this lesion has an ADC value of 1.314 × 10^{-3} mm^2/s, a D value of 1.760 × 10^{-3} mm^2/s and a K value of 0.746, respectively. ADC, apparent diffusion coefficient.

prognosis in patients with gastric cancers (6). We found that DKI derived kurtosis value of poorly/moderate-poorly differentiated gastric cancers was significantly higher than that of moderately/well differentiated tumors. We speculated that poorly differentiated gastric cancers usually present with markedly irregular architecture and cellular pleomorphism, leading to a more chaotic water molecular diffusion within the tissues. Since kurtosis is a parameter characterizing the deviation of water molecular diffusion from the Gaussian distribution, poorly differentiated lesions tended to show higher kurtosis values, which has been confirmed by multiple previous studies (20,22,23). For instance, Sun *et al.* reported that kurtosis of high-grade breast cancers was significantly higher than that of low-grade ones (P=0.001), and kurtosis correlated with histological grade positively (r =0.75) (23). And Zhu *et al.* demonstrated that high-grade rectal adenocarcinomas showed significantly higher kurtosis values than low-grade tumors, and kurtosis performed better than ADC in identifying high-grade rectal adenocarcinomas (20). In our study, kurtosis also showed a better performance in differentiating poorly/moderately-poorly from moderately/well differentiated gastric cancers compared with ADC (AUC =0.794 and 0.732, respectively).

Lauren classification is also an important prognostic factor of gastric cancers (5,31). We found that gastric cancers of diffuse type showed significantly higher kurtosis values than those of intestinal type. We speculated that gastric cancers of diffuse types were composed with multiple cellular components and less contact glandular structures, which led to more restrict and disordered Brownian motion of water molecules within tumor tissues and consequently an increased kurtosis value. In this study, kurtosis could differentiate gastric cancers of diffuse type from those of intestinal or mixed types with an AUC of 0.737.

T staging of gastric cancers also has a great influence on treatment and prognosis of those patients (32). We found that T3–T4 gastric cancers showed significantly lower ADC and diffusivity values but higher kurtosis values than T1–T2 lesions. As the T stage increased, the tumor extended

Table 1 The apparent diffusion coefficient, diffusivity (D) and kurtosis (K) values of gastric cancers with different histopathological features

Histological information	ADC	D	K
Differentiation degree			
Poorly/moderate-poorly	1.150±0.251	1.600±0.322	0.842±0.134
Moderately/well	1.360±0.279	1.786±0.380	0.709±0.084
Independent samples *t*-test	0.039†	0.154	0.002†
Lauren classification			
Diffuse	1.107±0.206	1.578±0.289	0.874±0.112
Mixed	1.170±0.257	1.574±0.253	0.811±0.185
Intestinal	1.309±0.312	1.742±0.421	0.745±0.104
ANOVA	0.057	0.272	0.010‡
T stage			
T1–T2	1.444±0.296	1.899±0.377	0.698±0.139
T3–T4	1.141±0.236	1.586±0.311	0.841±0.126
Independent samples *t*-test	0.004†	0.021†	0.009†
N stage			
N0	1.400±0.319	1.874±0.374	0.739±0.157
N1	1.123±0.302	1.543±0.412	0.847±0.154
N2	1.133±0.235	1.518±0.316	0.804±0.108
N3	1.155±0.217	1.636±0.269	0.850±0.130
ANOVA	0.086	0.102	0.224
N stage			
N0	1.400±0.319	1.874±0.374	0.739±0.157
N1–N3	1.142±0.234	1.583±0.310	0.836±0.128
Independent samples *t*-test	0.010†	0.023†	0.063
Vascular invasion			
Present	1.178±0.255	1.627±0.324	0.822±0.133
Absent	1.223±0.337	1.650±0.424	0.808±0.162
Independent samples *t*-test	0.682	0.872	0.801
Perineural invasion			
Present	1.164±0.237	1.610±0.303	0.829±0.127
Absent	1.265±0.356	1.710±0.449	0.788±0.171
Independent samples *t*-test	0.410	0.409	0.404

†, $P<0.05$ with independent samples *t*-test; ‡, $P<0.05$ with ANOVA. The ADC and D values are in unit of $\times 10^{-3}$ mm^2/s. ADC, apparent diffusion coefficient; ANOVA, one-way analysis of variance.

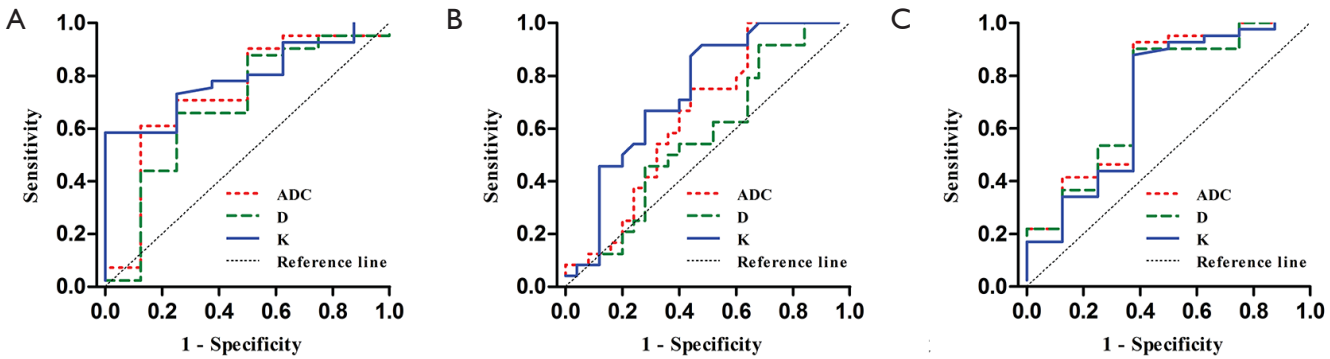

Figure 3 Graphs showing the diagnostic performance of the ADC, corrected diffusion coefficient (D) and diffusion kurtosis coefficient (K) values with ROC curve analysis. (A) ROC curves of the ADC, D and K values in differentiating poorly/moderate-poorly differentiated gastric cancers from moderately/well differentiated ones (area under the ROC curve, AUC =0.732, 0.683 and 0.794, respectively); (B) ROC curves of the ADC, D and K values in differentiating gastric cancers with diffuse type from mixed or intestinal type (AUC =0.649, 0.572 and 0.737, respectively); (C) ROC curves of the ADC, D and K values in differentiating gastric cancers at stage N1–N3 from those at stage N0 (AUC =0.741, 0.729 and 0.712, respectively). The reference line indicates random assignment. ROC, receiver operating characteristic; ADC, apparent diffusion coefficient.

Table 2 Diagnostic performance of the apparent diffusion coefficient, diffusivity (D) and kurtosis (K) values with receiver operating characteristic curve analysis

Types	Parameters	Cutoff	Sensitivity	Specificity	AUC	P value
Poorly/moderate-poorly	ADC	1.157	0.610	0.875	0.732	0.040†
	D	1.702	0.659	0.750	0.683	0.105
	K	0.826	0.585	1.000	0.794	0.009†
Diffuse type	ADC	1.490	1.000	0.360	0.649	0.073
	D	1.899	0.917	0.320	0.572	0.390
	K	0.742	0.917	0.520	0.737	0.004†
N+	ADC	1.494	0.927	0.625	0.741	0.033†
	D	1.909	0.902	0.625	0.729	0.042†
	K	0.699	0.878	0.625	0.712	0.060
Vascular invasion	ADC	1.461	0.833	0.429	0.517	0.886
	D	1.924	0.881	0.429	0.515	0.898
	K	0.719	0.810	0.429	0.529	0.808
Perineural invasion	ADC	1.526	0.949	0.400	0.573	0.480
	D	1.924	0.897	0.400	0.556	0.585
	K	0.734	0.821	0.500	0.587	0.399

†, P<0.05 with ROC curve analysis. The cutoff values with the largest Youden index (sensitivity + specificity −1) were calculated from the ROC curves. The ADC and D values are in unit of $\times 10^{-3}$ mm^2/s. N+, N1–N3 stage; ROC, receiver operating characteristic; AUC, area under the ROC curve; ADC, apparent diffusion coefficient.

Table 3 Correlations between the apparent diffusion coefficient diffusivity (D) and kurtosis (K) values with different histopathological features

Histological information	ADC	D	K
Differentiation degree			
r	0.372**	0.225	−0.481**
P value	0.009†	0.124	0.001†
Lauren classification			
r	0.287*	0.150	−0.388**
P value	0.048†	0.310	0.006†
T stage			
r	−0.394**	−0.322**	0.330**
P value	0.006†	0.026†	0.022†
N stage			
r	−0.205	−0.121	0.191
P value	0.161	0.413	0.192
Overall stage 1			
r	−0.341**	−0.263	0.306**
P value	0.018†	0.071	0.035†

†, P<0.05 with partial correlation test; *, weakly correlated; **, moderately correlated. ADC, apparent diffusion coefficient.

deeper into surrounding tissues with stronger ability of proliferation and invasion. Tumors showed increased cell density and nuclear to cytoplasmic ratio, leading to more restricted and disordered water molecular diffusion, causing decreased ADC and diffusivity and higher kurtosis values. Our previous study found that ADC values correlated negatively with postoperative T staging (12). However, the ADC values were calculated with mono-exponential model based on DWI using two b values. In this study, we obtained ADC and kurtosis values with a nonlinear model based on DKI using multiple b values, which were also correlated with postoperative T staging.

Lymph nodes metastasis has a great effect on treatment planning and prognosis prediction (33). However, accurate preoperative assessment of N stage remains a challenge in clinical practice. It was not surprising to found that the ADC and diffusivity values of gastric cancers with lymph nodes metastases were significantly lower than those without lymph nodes metastasis. The ADC and diffusivity values reflected microstructural features of gastric cancers, which indicate its aggressiveness indirectly. Especially ADC could predict lymph node status with an AUC of 0.741.

We failed to detect any significant differences of ADC, diffusivity and kurtosis values in gastric cancers with and without vascular or perineural invasion probably due to relatively small sample size or some inclusion bias, which required further study in the future.

In addition, our results showed that tumor volume had significant correlations with differentiation degree, Lauren classification, T stage, N stage and overall stage of gastric cancers, thus we analyzed the correlations between DKI parameters and different pathological characteristics of gastric cancers by using partial correlation test to remove the impact of tumor volume, which also showed significant correlations. This indicated that DKI parameters were helpful for assessing those pathological characteristics, whatever the tumor volume.

There were some limitations in this study. First, the sample size was relatively small and there might be some inclusion bias. Second, we simply draw ROIs within the solid part in the largest slice of the lesion without rigorous reference to postoperative specimens, and we will try whole-volume analysis in our next study. Third, the number and distribution of b values were arbitrarily selected for DKI sequence, which required optimization in the future.

In conclusion, we demonstrated that there were significant differences of kurtosis in gastric cancers with different differentiation degrees and Lauren types, and the ADC and diffusivity values differed significantly among gastric cancers at different T and overall stages. DKI derived parameters might be helpful in preoperative assessment of gastric cancer's aggressiveness, especially in identifying poorly/moderate-poorly differentiated or diffuse type gastric cancers, and in predicting the status of lymph nodes metastasis.

Acknowledgments

Funding: None.

Footnote

Provenance and Peer Review: This article was commissioned by the Guest Editors (Yì-Xiáng J. Wáng, Yong Wang) for the series "Translational Imaging in Cancer Patient Care" published in *Translational Cancer Research*. The article has

undergone external peer review.

Conflicts of Interest: All authors have completed the ICMJE uniform disclosure form (available at http://dx.doi.org/10.21037/tcr.2017.07.02). The series "Translational Imaging in Cancer Patient Care" was commissioned by the editorial office without any funding or sponsorship. The authors have no other conflicts of interest to declare.

Ethical Statement: The authors are accountable for all aspects of the work in ensuring that questions related to the accuracy or integrity of any part of the work are appropriately investigated and resolved. The study was conducted in accordance with the Declaration of Helsinki (as revised in 2013). This prospective study received the approval of local ethics committee. Written informed consent was obtained from each patient.

References

1. Torre LA, Bray F, Siegel RL, et al. Global cancer statistics, 2012. CA Cancer J Clin 2015;65:87-108.
2. Hartgrink HH, Jansen EP, van Grieken NC, et al. Gastric cancer. Lancet 2009;374:477-90.
3. Röcken C, Behrens HM. Validating the prognostic and discriminating value of the TNM-classification for gastric cancer - a critical appraisal. Eur J Cancer 2015;51:577-86.
4. Hwang JE, Hong JY, Kim JE, et al. Prognostic significance of the concomitant existence of lymphovascular and perineural invasion in locally advanced gastric cancer patients who underwent curative gastrectomy and adjuvant chemotherapy. Jpn J Clin Oncol 2015;45:541-6.
5. Qiu M, Zhou Y, Zhang X, et al. Lauren classification combined with HER2 status is a better prognostic factor in Chinese gastric cancer patients. BMC Cancer 2014;14:823.
6. Zu H, Wang H, Li C, et al. Clinicopathologic characteristics and prognostic value of various histological types in advanced gastric cancer. Int J Clin Exp Pathol 2014;7:5692-700.
7. Flucke U, Mönig SP, Baldus SE, et al. Differences between biopsy- or specimen-related Laurén and World Health Organization classification in gastric cancer. World J Surg 2002;26:137-40.
8. Lee IS, Park YS, Lee JH, et al. Pathologic discordance of differentiation between endoscopic biopsy and postoperative specimen in mucosal gastric adenocarcinomas. Ann Surg Oncol 2013;20:4231-7.
9. Jang KM, Kim SH, Lee SJ, et al. Upper abdominal gadoxetic acid-enhanced and diffusion-weighted MRI for the detection of gastric cancer: Comparison with two-dimensional multidetector row CT. Clin Radiol 2014;69:827-35.
10. Huo X, Yuan K, Shen Y, et al. Clinical value of magnetic resonance imaging in preoperative T staging of gastric cancer and postoperative pathological diagnosis. Oncol Lett 2014;8:275-80.
11. Joo I, Lee JM, Kim JH, et al. Prospective comparison of 3T MRI with diffusion-weighted imaging and MDCT for the preoperative TNM staging of gastric cancer. J Magn Reson Imaging 2015;41:814-21.
12. Liu S, Wang H, Guan W, et al. Preoperative apparent diffusion coefficient value of gastric cancer by diffusion-weighted imaging: Correlations with postoperative TNM staging. J Magn Reson Imaging 2015;42:837-43.
13. He J, Shi H, Zhou Z, Chen J, et al. Correlation between apparent diffusion coefficients and HER2 status in gastric cancers: pilot study. BMC Cancer 2015;15:749.
14. Liu S, Guan W, Wang H, et al. Apparent diffusion coefficient value of gastric cancer by diffusion-weighted imaging: correlations with the histological differentiation and Lauren classification. Eur J Radiol 2014;83:2122-8.
15. Giganti F, Orsenigo E, Esposito A, et al. Prognostic Role of Diffusion-weighted MR Imaging for Resectable Gastric Cancer. Radiology 2015;276:444-52.
16. Eghtedari M, Ma J, Fox P, et al. Effects of magnetic field strength and b value on the sensitivity and specificity of quantitative breast diffusion-weighted MRI. Quant Imaging Med Surg 2016;6:374-80.
17. Li YT, Cercueil JP, Yuan J, et al. Liver intravoxel incoherent motion (IVIM) magnetic resonance imaging: a comprehensive review of published data on normal values and applications for fibrosis and tumor evaluation. Quant Imaging Med Surg 2017;7:59-78.
18. Yuan J, Lo G, King AD. Functional magnetic resonance

imaging techniques and their development for radiation therapy planning and monitoring in the head and neck cancers. Quant Imaging Med Surg 2016;6:430-48.
19. Yuan J, Wong OL, Lo GG, et al. Statistical assessment of bi-exponential diffusion weighted imaging signal characteristics induced by intravoxel incoherent motion in malignant breast tumors. Quant Imaging Med Surg 2016;6:418-29.
20. Zhu L, Pan Z, Ma Q, et al. Diffusion Kurtosis Imaging Study of Rectal Adenocarcinoma Associated with Histopathologic Prognostic Factors: Preliminary Findings. Radiology 2017;284:66-76.
21. Jensen JH, Helpern JA, Ramani A, et al. Diffusional kurtosis imaging: the quantification of non-gaussian water diffusion by means of magnetic resonance imaging. Magn Reson Med 2005;53:1432-40.
22. Bai Y, Lin Y, Tian J, et al. Grading of Gliomas by Using Monoexponential, Biexponential, and Stretched Exponential Diffusion-weighted MR Imaging and Diffusion Kurtosis MR Imaging. Radiology 2016;278:496-504.
23. Sun K, Chen X, Chai W, et al. Breast Cancer: Diffusion Kurtosis MR Imaging-Diagnostic Accuracy and Correlation with Clinical-Pathologic Factors. Radiology 2015;277:46-55.
24. Wang Q, Li H, Yan X, et al. Histogram analysis of diffusion kurtosis magnetic resonance imaging in differentiation of pathologic Gleason grade of prostate cancer. Urol Oncol 2015;33:337.e15-24.
25. Suo S, Chen X, Ji X, et al. Investigation of the non-Gaussian water diffusion properties in bladder cancer using diffusion kurtosis imaging: a preliminary study. J Comput Assist Tomogr 2015;39:281-5.
26. Yu J, Xu Q, Song JC, et al. The value of diffusion kurtosis magnetic resonance imaging for assessing treatment response of neoadjuvant chemoradiotherapy in locally advanced rectal cancer. Eur Radiol 2017;27:1848-57.
27. Jiang JX, Tang ZH, Zhong YF, et al. Diffusion kurtosis imaging for differentiating between the benign and malignant sinonasal lesions. J Magn Reson Imaging 2017;45:1446-54.
28. Zhang XP, Tang L, Sun YS, et al. Sandwich sign of Borrmann type 4 gastric cancer on diffusion-weighted magnetic resonance imaging. Eur J Radiol 2012;81:2481-6.
29. Zhang J, Zhou Y, Jiang K, et al. Evaluation of the seventh AJCC TNM staging system for gastric cancer: a meta-analysis of cohort studies. Tumour Biol 2014;35:8525-32.
30. Lauwers GY, Carneiro F, Graham DY, et al. Gastric carcinoma. In: Bosman FT, Carneiro F, Hruban RH, et al. editors. WHO classification of tumors of the digestive system. Lyon, France: IARC Press, 2010:225-7.
31. Chen YC, Fang WL, Wang RF, et al. Clinicopathological Variation of Lauren Classification in Gastric Cancer. Pathol Oncol Res 2016;22:197-202.
32. Yasuda K, Shiraishi N, Inomata M, et al. Prognostic significance of macroscopic serosal invasion in advanced gastric cancer. Hepatogastroenterology 2007;54:2028-31.
33. Sekiguchi M, Oda I, Taniguchi H, et al. Risk stratification and predictive risk-scoring model for lymph node metastasis in early gastric cancer. J Gastroenterol 2016;51:961-70.

Cite this article as: Ji C, Zhang Y, Zheng H, Chen L, Guan W, Guo T, Zhang Q, Liu S, He J, Zhou Z. Diffusion kurtosis imaging in assessment of gastric cancer aggressiveness. Transl Cancer Res 2017;6(6):1032-1042. doi: 10.21037/tcr.2017.07.02

Supplementary

Table S1 The clinicopathological characteristics of the patients with gastric cancers

Characteristics	No. of patients	Percentage (%)
Gender		
Male	31	63.3
Female	18	36.7
Age (years)		
<60	17	34.7
≥60	32	65.3
Location		
Cardia	13	26.5
Body	15	30.7
Antrum	13	26.5
Cardia + body	2	4.1
Body + antrum	3	6.1
Cardia + body + antrum	3	6.1
Pathological type		
Ade	31	63.2
Pcc	10	20.4
Muc	2	4.1
Ade + Pcc	4	8.2
Ade + Pcc+ Muc	2	4.1
Differentiation degree		
Poorly	31	63.3
Moderate-poorly	10	20.4
Moderately	6	12.2
Well	2	4.1
Lauren classification		
Intestinal	16	32.6
Mixed	9	18.4
Diffuse	24	49.0
T stage		
T1	3	6.1
T2	4	8.2
T3	31	63.3
T4	11	22.4
N stage		
N0	8	16.3
N1	8	16.3
N2	12	24.5
N3	21	42.9
Overall stage		
I	3	6.1
II	9	18.4
III	34	69.4
IV	3	6.1
Lymph node metastasis		
Present	41	83.7
Absent	8	16.3
Vascular invasion		
Present	42	85.7
Absent	7	14.3
Perineural invasion		
Present	39	79.6
Absent	10	20.4

Ade, tubular/papillary adenocarcinoma; Pcc, poorly cohesive carcinoma; Muc, mucinous adenocarcinoma.